ECS Journal of Solid State Science and Technology, **2** (1) Q23-Q26 (2013)
2162-8769/2013/2(1)/Q23/4/$28.00 © The Electrochemical Society

Exploiting Water-Mediated Ethanol Sensing by Polycrystalline ZnO at Room Temperature

Jiaqi Cheng, Muhammad Asim Rasheed,[a] and Kristin M. Poduska[*,z]

Departments of Chemistry & Physics and Physical Oceanography, Memorial University of Newfoundland, St. John's, NL A1B 3X7, Canada

Ambient moisture can dramatically promote the response of ZnO to ethanol vapor, a hydrophilic gas. By comparing sensor responses in a broad range of humidities, we show that there is a consistent enhancement in ethanol adsorption on ZnO when physisorbed water, detected by capacitance measurements, is present. The time constants related to the capacitive signal recovery during desorption are consistent with the formation of C_2H_5OH-$(H_2O)_n$ clusters that have a different desorption rate than water alone. These room temperature results indicate that surface water mediates the dynamic adsorption/re-evaporation equilibrium of solvated ethanol molecules. Thus, attention to interactions between the target gas molecules and their environment is important for understanding the mechanisms behind selective gas sensing.
 [DOI: 10.1149/2.019301jss]

Manuscript submitted August 28, 2012; revised manuscript received October 12, 2012. Published November 16, 2012.

Moisture is always present in ambient environments, so an understanding of water-solid interactions is important in many applied fields such as corrosion, catalysis, and sensor development.[1] The surface structure and reactivity of semiconducting metal oxides (MOX) such as ZnO, SnO_2 and WO_3 have been studied extensively for electrical gas sensing applications. These materials have highly sensitive electrical conductivity and capacitance responses to many gaseous species including CO, NH_3, and volatile organic compounds (VOCs) while having low production costs and high thermal durability.[2] However, the presence of environmental H_2O can effectively alter the reactivities of MOX surfaces, which leads to difficulties in obtaining reliable and selective sensing signals for different target gases in real-world environments.[3–6]

Most investigations on the gas sensing performance of MOX materials have focused on analyte gas detection at relatively high operating temperatures (500–800 K), where optimal sensing responses are normally reached.[7] This is because the formation of surface hydroxyls from chemisorptive water dissociation tends to dominate at these high temperatures, and the net conductivity changes are determined by surface characteristics such as oxygen species density, surface defects and hydroxyl coverage.[1] At these high temperatures, target gas molecules undergo a combustive type of reaction that yields oxidized or reduced species on the MOX surface.[8] In contrast, at low temperatures ($\leq$ 400 K), physisorbed water in its molecular form can increase the surface conductivity by donating lone pair electrons to the oxide's space charge region. There is surprisingly little work that focuses on water effects on gas-sensing of MOX at room temperature, despite the urgent need for room temperature gas sensors.[9] Polymeric sensors are typically preferred at ambient temperatures, but they can also be adversely affected by the presence of moisture, and they exhibit similar selectivity challenges to those encountered in MOX sensors.

In this study, we show that ambient moisture can dramatically promote the response of ZnO to ethanol (EtOH) vapor, a hydrophilic gas. By comparing sensor recovery times in a broad range of humidities, we show that there is an enhancement of ethanol adsorption on ZnO when it is covered with a physisorbed water layer, whose thickness depends on the relative humidity (RH) of the atmosphere around it. Capacitance data allow us to infer the formation of ethanol-water critical clusters, and we demonstrate that there is discrimination of sensing events between ethanol vapor and background humidity. Our results show that paying more attention to interactions between the target gas molecules and their environment could offer benefits for developing more selective gas sensing materials.

Experimental

Synthesis.— ZnO particles were synthesized using a room temperature solid-state metathesis reaction.[10] All reagents were analytical grade (99%) and used without further purification. $ZnCl_2$ (Caledon) and NaOH (EM Science) were ground separately to fine powders, then mixed together in a beaker with a molar ratio of 1:2 to react in the following way:

$$ZnCl_2 + 2NaOH \rightarrow Zn(OH)_2 + 2NaCl \quad (1)$$

$$Zn(OH)_2 \rightarrow ZnO + H_2O \quad (2)$$

Within 2 minutes of stirring the solid mixture, there was heat release and generation of water vapor, as well as a color change from white to yellow, and then back to white within tens of seconds after the reaction finished. The product was washed with ultrapure water (Barnstead Nanopure 18.2 Ω·cm) several times to remove the NaCl by-product, and then dried in an oven at 350 K before further characterization.

Material characterization.— X-Ray diffraction (XRD) and Fourier transform infrared spectroscopy (FTIR) were used to assess the crystallinity and phase composition of the dried product. XRD data were collected with a Rigaku Ultima IV X-ray diffractometer (Cu K_α, 3°/min, step size 0.02° 2θ), and lattice constant refinements were performed with Jade software (Materials Data Inc.). FTIR data were collected in transmission mode with a Bruker Alpha at 4 cm^{-1} resolution on specimens dispersed in a 7 mm diameter KBr pellet. Representative XRD data, shown in Fig. 1a, indicate that the product is highly crystalline with lattice constants of $a = (3.5252 \pm 0.001)$ Å and $c = (5.210 \pm 0.001)$ Å, which are appropriate for wurtzite-type ZnO (JCPDS 36-1451, with $a = 3.250$ Å and $c = 5.207$ Å). No evidence of secondary phases was detected, either in XRD data or in FTIR spectra (Fig. 1b). Estimates of particle sizes were obtained by dynamic light scattering methods (Malvern Zetasizer Nano ZS) and confirmed qualitatively from scanning electron microscopy (SEM) images (FEI Quanta 400) of dispersed ZnO particles coated with a conductive carbon layer. Fig. 1c shows typical particle aggregates with poorly developed facets and diameters ~100 nm. These sizes are consistent with the particle size estimates obtained from light scattering measurements (110 ± 30 nm). Brunauer-Emment-Teller (BET) analyses yield an average surface area of 3.6 ± 0.3 m^2g^{-1}. X-ray Photoelectron Spectra (XPS) data collected with a VG Microtech Multi-Lab ESCA 2000 indicate O atom binding energies that are consistent with ZnO that has a thin (≤5 nm) layer of surface hydroxyl groups present.[11]

Gas sensing measurement.— Thick films (120 ± 30 μm) of ZnO particles served as sensor materials for subsequent study. A slurry of the as-prepared ZnO powder (0.10 g dispersed in 2 mL of acetone and

[*]Electrochemical Society Active Member.
[a]Present address: Department of Metallurgy and Materials Engineering, Pakistan Institute of Engineering and Applied Sciences, Islamabad 45650, Pakistan.
[z]E-mail: kris@mun.ca; www.physics.mun.ca/~kris

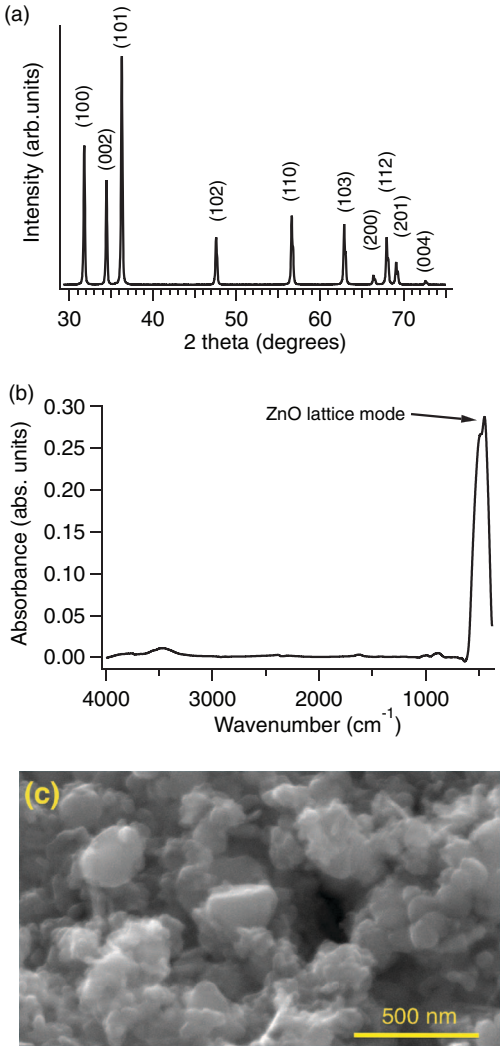

Figure 1. (a) Representative XRD data with all peaks indexed to wurtzite-type ZnO. (b) Representative FTIR data show a characteristic ZnO lattice mode peak near 450 cm^{-1}. (c) SEM image of ZnO particles.

sonicated for 30 s) was slowly poured onto, and spread evenly over, a mechanically polished stainless steel strip. The steel strip served as one electrode for subsequent electrical measurements, and the second electrode was a stainless steel pressure contact on the top of the film. For films with 1 cm × 7 cm area, typical resistance and capacitance values were ∼20 MΩ and ∼100 pF, respectively, at 45% ambient RH.

Prior to use, each sensor film was equilibrated in a sealed chamber (25 cm × 25 cm × 25 cm), and Ohmic electrical contacts were made with mechanically polished steel (0.5 cm^2). RH levels inside the test chamber were controlled and modified using different saturated salts solutions. At 295 K, 150 mL of one of the following saturated salt solutions yields a distinct and characteristic relative humidity: CH_3CO_2K (20 ± 2%), K_2CO_3 (45 ± 2%), or KNO_3 (90 ± 2%).[12] Before initiating gas detection measurements, one of the aforementioned salt solutions was kept in the chamber for two hours to reach the intended equilibrium RH. Our experiments utilized independent control of the RH of the target gas as well. For clarity of presentation in the rest of this manuscript, the humidity levels of the target gases – ethanol-water vapor mixtures – are categorized as "dry" (20% RH), "medium" (45% RH), or "wet" (90% RH).

Gas sensing experiments were initiated by injecting 20 mL of the target gas into the chamber in close proximity to the sensing film. Given the large chamber volume relative to that of the injected gas, multiple injections could be executed without interference from one injection to the next. EtOH concentrations were calculated using the standard vapor pressure of anhydrous ethanol (ACS grade) under atmospheric pressure at 294 K. We note that this method of determining gas concentration is more realistic, and more conservative, than some other reports of ethanol sensing by ZnO.[13] All of our experiments used EtOH vapor at 5000 ppm unless otherwise noted.

Sensing responses for the ZnO films were assessed by measuring capacitance changes at 3 kHz with an applied AC RMS voltage of 50 mV (National Instruments LCR meter with PXI-1033 interface). We interpret the response assuming that our films function as parallel plate capacitors such that $C = A\epsilon_0\epsilon/d$, where C is the effective capacitance, ϵ_0 is the permittivity of free space, A is the total contact area of the plate, ϵ is the effective dielectric constant of the thin film.[14] Since ϵ changes with humidity, and with exposure to target gases such as ethanol, the resulting change in capacitance yields a measurable response. We report the response $S = (C_g - C_a)/C_a$, where C_g is the maximum capacitance response after exposure to the target gas, and C_a is the baseline capacitance value. The recovery time τ is extracted from an exponential fit of the sensor's return to baseline (after exposure to the target gas) and corresponds to the time required to return within 95% of the original (baseline) capacitance. All sensing studies were conducted at room temperature (295 ± 2 K).

Results and Discussion

Response enhancement with humidity.— Increasing ambient humidity causes a significant increase in the ZnO response to ethanol vapor. A representative example of this effect is shown Fig. 2a, which compares sensor capacitance responses triggered by a series of four identical ethanol vapor injections (5000 ppm in a 45% RH target gas) at ambient (test chamber) RH values of 20%, 45% and 90%. The dotted lines indicate the time at which the target gas was introduced

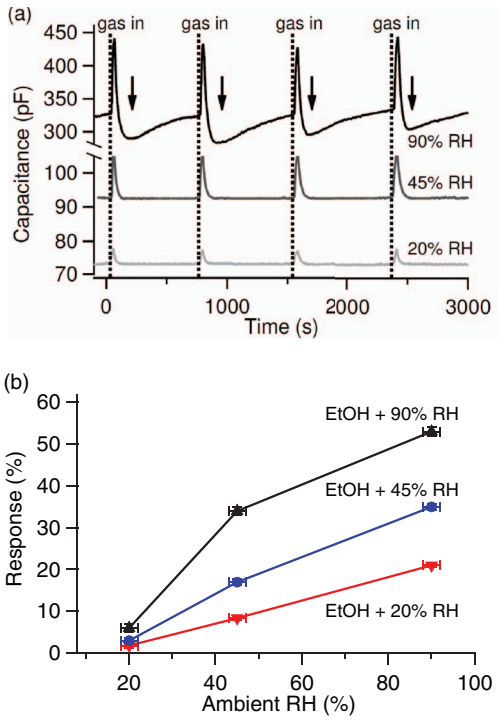

Figure 2. (a) A representative comparison of sensor capacitance responses triggered by ethanol vapor injections (5000 ppm in a 45% RH target gas) at ambient (test chamber) RH values of 20%, 45% and 90%. (b) ZnO response to EtOH increases with both increasing ambient RH and increasing target gas RH. The lines connecting the data points serve as guides to the eye, and uncertainty estimates are displayed for each data point.

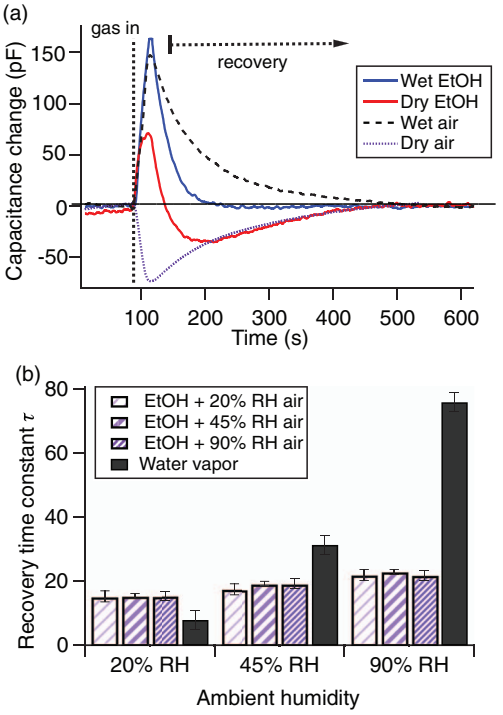

Figure 3. (a) Comparison of representative capacitive signals of ZnO when sensing dry air (20% RH), wet air (100% RH), dry ethanol vapor (5000 ppm at 20%), or wet ethanol vapor (5000 ppm at 90% RH) in a test chamber held at 90% ambient RH. (b) Comparison of sensor recovery times after exposure to target gases with different humidities in test chamber environments with a range of different ambient humidities.

to the sensor. Both the baseline (resting) capacitance values and the magnitudes of the sensing responses increase with increasing ambient humidity. The arrows indicate the below-baseline recovery that occurs when the target gas has a RH that is much lower than the ambient RH. Fig. 2b shows that ZnO response to EtOH increases with both increasing ambient RH and increasing target gas RH over the full range of ambient and target gas RH combinations. We note that the poor response of ZnO to ethanol vapor in a dry environment is consistent with previous investigations.[6,13,15–17]

It is well known that at room temperature, a solid surface in air will adsorb many layers of water, leading to formation of a thin condensed water layer on the surface whose thickness equilibrates with ambient RH.[18] Since water has dielectric constant of 80, while that for ZnO is 10, an absorbed water layer will increase the effective film capacitance. Our experiments show evidence of this changing water layer thickness in the capacitance baseline of the sensor, since at resting value (with no target gas present), the capacitance increases with increasing ambient RH. For example, Fig. 2a shows that an ambient RH value of 20% registers a baseline capacitance near 70 pF, while an ambient RH of 90% increases the baseline above 300 pF.

Desorption of water and ethanol hydrates.— Despite the synergistic effect of water and EtOH in the ZnO response, it is also possible to discriminate between EtOH and H_2O sensing events by analyzing the time required for the measured capacitance to return to its baseline value after exposure to a pulse of the target gas. We compared representative sensing signals of four target gases (dry ethanol (20% RH), wet ethanol (90% RH), dry air (20% RH) and water vapor (100% RH)) in humid (90% RH) ambient conditions where there will be a high level of surface water on ZnO. Fig. 3a shows that, under these conditions, ethanol vapor and water vapor target gases behave in qualitatively different ways. EtOH (whether dry or wet) always gives a capacitance *increase*. On the other hand, the response in the absence of ethanol (RH-controlled air only) appears to depend on the fugitive

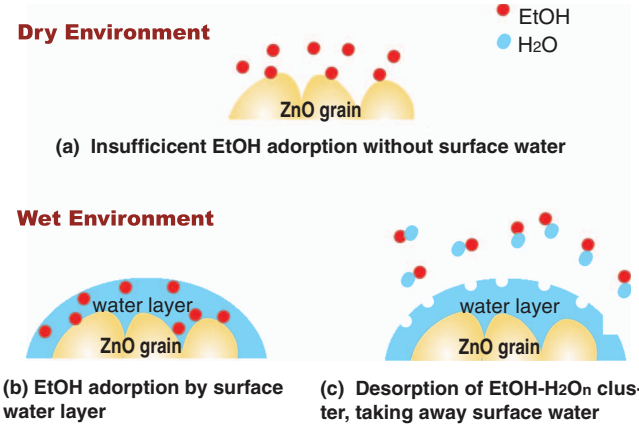

Figure 4. Schematic diagram depicting the ethanol sensing processes by ZnO grains under (a) dry and (b) wet ambient RH conditions. (c) When the ambient RH is high, EtOH desorbs as a complex with water, thereby temporarily depleting some of the surface water.

buildup (or removal) of the condensed thin water layer on the ZnO surface. Thus, an *increase* in capacitance occurs when the RH of the target gas is higher than ambient, while a *decrease* occurs when the target gas that is drier than ambient. An extreme example of this effect is the "over-recovery" that occurs during when a relatively dry target gas is directed on the ZnO film, as indicated with arrows in Fig. 2a. We infer from this behavior that the dry EtOH removes water molecules from the ZnO surface in order to form EtOH-H_2O clusters, and then atmospheric water vapor must be reabsorbed to equilibrate the ZnO surface water.

Solvation of EtOH has been heavily investigated for its fundamental non-ideal behavior of mixing that is caused by a hydrogen-bonded H_2O-EtOH network. Many studies have shown that when ethanol vapor interacts with surface water, a cluster of C_2H_5OH-$(H_2O)_n$ with a critical size ($1 \leq n \leq 3$) will form at the gas-liquid interfaces.[19] For example, Katrib et al. investigated the composition and geometry of ethanol-water clusters during the ethanol vapor uptake process by water, and their experimental and theoretical results show that the interaction of one water molecule with ethanol ($n = 1$) is favored.[20]

At this stage, we are not able to confirm the exact structure of the ethanol hydrate that desorbs from our ZnO surfaces. However, evidence for the existence of ethanol hydrates was derived from the signal recovery time constant. Assuming first-order desorption kinetics,[21] we fitted the signal recovery curves of all sensing data with a single exponential function to extract the recovery constant. What is surprising in the data trend shown in Fig. 3b is that the recovery constant for EtOH – for any combination of target gas and ambient RH value – is identical, despite the fact that the sensor response is strongly affected by ambient RH (as shown in Fig. 2b). This again suggests that ethanol-water association on the ZnO surface leads to the formation of a cluster whose desorption rate is independent of the ambient water pressure.

In contrast, for water vapor alone, the recovery time constant increases with an increasing ambient RH (Fig. 3b). We believe this is due to slower desorption of water from ZnO surface with higher water vapor pressure in the surrounding environment.[22]

A schematic overview of the ethanol-hydrate-based sensing mechanism for ZnO at room temperature is depicted schematically in Fig. 4. Limited response to ethanol at low RH is due to the low adsorption affinity between ethanol and a dry ZnO surface (Fig. 4). For high ambient RH, however, the adsorption efficiency of ethanol onto ZnO surface can be enhanced by solvation by a surface water layer to form ethanol-water clusters (Fig. 4b). When desorption occurs, surface water molecules that have become part of the EtOH-water clusters are removed, thereby thinning the water layer which results in a drop of sensor capacitance below the original starting (baseline) value

(Fig. 4c). (The experimental observation of this water removal appears as a capacitance decrease below the original baseline level, as indicated by the arrows in Fig. 2a). We note that this below-baseline recovery effect is less predominant when the humidity level of the incident ethanol vapor is comparable to that of the surrounding environment.

To confirm the validity of this water-mediated room temperature sensing mechanism, we executed control experiments by testing different hydrophobic vapors, including methane, hexane, and benzene. Each of these gases has been reported as detectable by ZnO-based gas sensors at higher temperatures (500–800 K),[23–25] but no sensing data are reported at room temperature. In our room temperature experiments, none of these vapors show a discernible capacitance response for any level of ambient or target gas humidity. This suggests that room temperature response depends critically on the solubility of the target gas in water. We also executed other control experiments wherein, using other synthetic methods,[26,27] we made several types of ZnO particles with different size distributions ranging from ∼5 nm to ∼2 μm. Regardless of the ZnO synthesis method, we observed similar trends in RH effects at room temperature, including increased response to EtOH for higher ambient RH as well as RH-independent recovery time constants for EtOH sensing.

Conclusions

Lack of selectivity is a common drawback of metal oxide gas sensors, but our data show that the response of dry air is qualitatively different, and there are quantitative differences in the recovery times between wet air and the ethanol-containing test gases. The recovery time for EtOH sensing is similar for all target gas and ambient humidities. However, more humid environments show a slower sensor recovery after exposure to either 20% or 100% RH air alone, due to drying and subsequent rehydration of the ZnO surface. Thus, tailoring the interaction between the target gas and ambient water vapor can simultaneously help improve sensor response and promote selectivity to hydrophilic ethanol gas at room temperature.

Acknowledgments

Natural Science and Engineering Resource Council (Canada), Petroleum Research Atlantic Canada, and the Canada Foundation for Innovation (New Opportunities) funded this work. We also acknowledge Dr. W. Aylward (XRD, grain size analyzer) and Dr. M. Shaffer (SEM) for use of their facilities through Memorial University's Core Research Equipment and Instrument Training network, Ms. J. Wen and Prof. A. Chen for BET measurements at Lakehead University (Thunder Bay, Ontario, Canada) and Dr. Z. Bayindir at the Dalhousie University Facilities for Materials Characterization managed by the Institute for Research in Materials (funded by the Atlantic Innovation Fund and other partners).

References

1. M. A. Henderson, *Surf. Sci. Rep.*, **46**, 1 (2002).
2. A. Oprea, N. Bârsan, and U. Weimar, *Sens. Actuat. B*, **142**, 470 (2009).
3. R. Binions, H. Davies, A. Afonja, S. Dungey, D. Lewis, D. E. Williams, and I. P. Parkin, *J. Electrochem. Soc.*, **156**, J46 (2009).
4. J. D. Prades, F. Hernández-Ramírez, T. Fischer, M. Hoffmann, R. Müller, N. López, S. Mathur, and J. R. Morante, *Appl. Phys. Lett.*, **97**, 243105 (2010).
5. Q. Qi, T. Zhang, X. Zheng, H. Fan, L. Liu, R. Wang, and Y. Zeng, *Sens. Actuat. B*, **134**, 36 (2008).
6. Z. Bai, C. Xie, M. Hu, S. Zhang, and D. Zeng, *Mater. Sci. Eng. B*, **149**, 12 (2008).
7. N. Barsan, D. Koziej, and U. Weimar, *Sens. Actuat. B*, **121**, 18 (2007).
8. G. H. Jain, *Proceedings of the Fifth International Conference on Sensing Technology 2011* (IEEE, Palmerston, New Zealand, 2011) pp. 66–72.
9. N. Yamazoe, *Sens. Actuat. B*, **108**, 2 (2005).
10. Y. Cao, P. Hu, W. Pan, Y. Huang, and D. Jia, *Sens. Actuat. B*, **134**, 462 (2008).
11. J. Lu, K. M. Ng, and S. Yang, *Ind. Eng. Chem. Res.*, **47**, 1095 (2008).
12. L. B. Rockland, *Anal. Chem.*, **32**, 1375 (1960).
13. X. Zhou, J. Li, M. Ma, and Q. Xue, *Physica E*, **43**, 1056 (2011).
14. T. T. Grove, M. F. Masters, and R. E. Miers, *Am. J. Phys.*, **73**, 52 (2005).
15. Y. J. Chen, C. L. Zhu, and G. Xiao, *Sens. Actuat. B*, **129**, 639 (2008).
16. Y. Chen, C. L. Zhu, and G. Xiao, *Nanotechnology*, **17**, 4537 (2006).
17. Q. Wan, Q. H. Li, Y. J. Chen, T. H. Wang, X. L. He, J. P. Li, and C. L. Lin, *Appl. Phys. Lett.*, **84**, 3654 (2004).
18. T. E. Graedel and C. Leygraf, *ECS Interface*, **10**, 24 (2001).
19. P. Davidovits, C. E. Kolb, L. R. Williams, J. T. Jayne, and D. R. Worsnop, *Chem. Rev.*, **111**, PR76 (2011).
20. Y. Katrib, Ph. Mirabel, S. Le Calvé, G. Weck, and E. Kochanski, *J. Phys. Chem. B*, **106**, 7237 (2002).
21. A. Fort, M. Mugnaini, I. Pasquini, S. Rocchi, and V. Vignoli, *Sens. Actuat. B*, **159**, 82 (2011).
22. Z. Chen and C. Lu, *Sens. Lett.*, **3**, 274 (2005).
23. B. L. Zhu, C. S. Xie, A. H. Wang, D. W. Zeng, W. L. Song, and X. Z. Zhao, *Mater. Lett.*, **59**, 1004 (2005).
24. S. Tian, F. Yang, D. Zeng, and C. Xie, *J. Phys. Chem. C*, **116**, 10586 (2012).
25. P. K. Basu, P. Bhattacharyya, N. Saha, H. Saha, and S. Basu, *Sens. Actuat. B*, **133**, 357 (2008).
26. T. Xu, X. Zhou, Z. Jiang, Q. Kuang, Z. Xie, and L. Zheng, *Cryst. Growth Des.*, **9**, 192 (2009).
27. J. Gupta, K. C. Barick, and D. Bahadur, *J. Alloys Compd.*, **509**, 6725 (2011).